Article
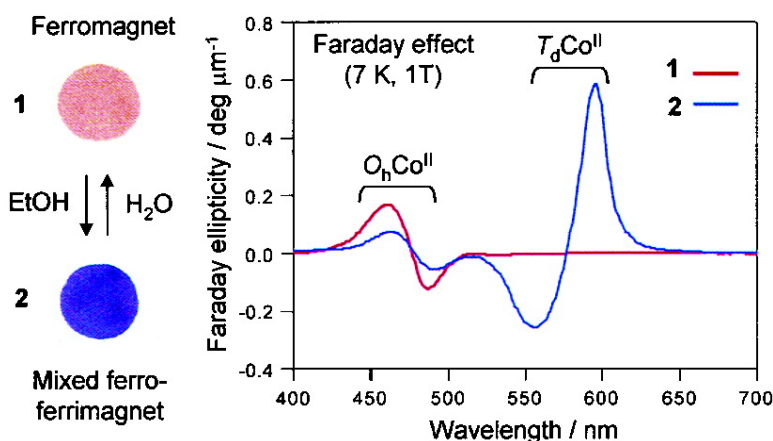
Solvatomagnetism-Induced Faraday Effect in a Cobalt Hexacyanochromate-Based Magnet

Yusuke Sato, Shin-ichi Ohkoshi, Ken-ichi Arai, Masanori Tozawa, and Kazuhito Hashimoto

More About This Article

Additional resources and features associated with this article are available within the HTML version:

- Supporting Information
- Links to the 16 articles that cite this article, as of the time of this article download
- Access to high resolution figures
- Links to articles and content related to this article
- Copyright permission to reproduce figures and/or text from this article

View the Full Text HTML

Solvatomagnetism-Induced Faraday Effect in a Cobalt Hexacyanochromate-Based Magnet

Yusuke Sato,[†] Shin-ichi Ohkoshi,*,[†,‡] Ken-ichi Arai,[†] Masanori Tozawa,[†] and Kazuhito Hashimoto*,[†]

Contribution from the Research Center for Advanced Science and Technology, The University of Tokyo, 4-6-1 Komaba, Meguroku, Tokyo 153-8904, Japan and PRESTO, JST, 4-1-8 Honcho Kawaguchi, Saitama, Japan

Received June 23, 2003; E-mail: ohkoshi@fchem.chem.t.u-tokyo.ac.jp; kazuhito@fchem.chem.t.u-tokyo.ac.jp

Abstract: Solvent exchange caused reversible variations in color, magnetic properties, and the Faraday spectra of $Co^{II}_{1.5}[Cr^{III}(CN)_6] \cdot 7.5H_2O$ (**1**) prepared in water. Compound **1** turned from peach to deep blue, which was due to a change in the coordination geometry on Co^{II} ion from six-coordinate pseudo-octahedral ($O_h Co^{II}$) to four-coordinate pseudo-tetrahedral ($T_d Co^{II}$) geometries, when it was immersed in EtOH. The confirmed formula for the deep blue powder was $Co^{II}_{1.5}[Cr^{III}(CN)_6] \cdot 2.5H_2O \cdot 2.0EtOH$. The magnetic properties also changed; that is, the magnetic critical temperature, saturation magnetization, and coercive field went from 25 to 18 K, from 7.0 to 5.5 μ_B, and from 240 to 120 G, respectively. This solvatomagnetism is because the ferromagnetic magnetic coupling between $O_h Co^{II}$ ($S = {}^3/_2$) and Cr^{III} ($S = {}^3/_2$) is replaced by the antiferromagnetic coupling between $T_d Co^{II}$ ($S = {}^3/_2$) and Cr^{III} ($S = {}^3/_2$). Accompanying the solvatochromism and solvatomagnetism, the Faraday spectra drastically changed. The Faraday ellipticity (FE) spectrum of **1** had a distorted dispersive peak (**A**), which is due to the $^4T_{1g} \rightarrow {}^4T_{1g}, {}^2T_{1g}$ transitions of $O_h Co^{II}$ ion, around 480 nm, but the FE spectra of **2** showed a new dispersive-shaped band (**B**) at 580 nm. The observed **B** band was assigned to the $^4A_2 \rightarrow {}^4T_2$ transition of the $T_d Co^{II}$ ion. The Faraday spectra were well reproduced by a simulation that considers the ligand field splitting, spin−orbital coupling, and the ferromagnetic ordering. These solvatochromic effects were repeatedly observed.

1. Introduction

The Faraday effect is a magneto-optical phenomenon that plays an important role in optical devices, such as optical isolator and optical circulator.[1] Since crystalline- and film-type molecule-based magnets[2] often possess transparently bright colors, they have a possibility of exhibiting a strong Faraday effect at a particular wavelength in the visible region. The reports of transparent magnetic materials have been limited to a few inorganic materials such as $FeBO_3$ and K_2CrCl_4.[3] From this viewpoint, we have studied the Faraday effect of Prussian blue analogues at the ferromagnetic state, using vanadium hexacyanochromates with a magnetic ordering temperature of 340 K.[4] Since then, the Faraday effect has been observed in several

molecule-based magnets.[5] In molecule-based magnets, the structure and magnetic properties can be controlled by a small change of circumstance. For example, Awaga et al. reported a reversible change between paramagnetism and weak ferromagnetism due to a solvatochromic behavior in a copper hydroxide intercalation compound.[6] This feature allows chemical modifications to control the magneto-optical effect. The objective in this work is to observe a new magneto-optical functionality, solvatomagnetism-induced magneto-optical effect. Typical magnetic materials such as metal alloys and metal oxides do not display this type of magneto-optical effect because they are not very sensitive to their environment. Among the solvatochromic effects, the color change of a solution of Co^{II} ion, which is caused by changing the coordination geometry around Co^{II} (6-coordinate octahedral ↔ 4-coordinate tetrahedral), is one of the famous phenomena.[7,8] Cobalt hexacyanochromate is reported to show ferromagnetism with a Curie temperature (T_C) of

† The University of Tokyo.
‡ PRESTO, JST.
(1) (a) Zvezdin, A. K.; Kotov, V. A. *Modern Magnetooptics and magnetooptical materials*; IOP: Bristol, Philadelphia, 1997. (b) Mallinson, J. C. *The Foundation of Magnetic Recording*; Academic Press: New York, 1993. (c) Sugano, S.; Kojima, N. *Magneto-Optics*; Springer-Verlag: Berlin, 2000.
(2) (a) Miller, J. S.; Epstein, A. J. *Angew. Chem., Int. Ed. Engl.* **1994**, *33*, 385. (b) Kahn, O. *Molecular Magnetism*; VCH: New York, 1993. (c) Gatteschi, D., Kahn, O., Miller, J. S., Palacio, F., Eds. *Magnetic Molecular Materials*; Kluwer: Dordrecht, the Netherlands, 1991. (d) Day, P., Underhill, A. E., Eds. Metal-Organic and Organic Molecular Magnets. *Philos. Trans. R. Soc. London, Ser. A* **1999**, *357*, 2851.
(3) (a) Wolfe, R.; Kurtzig, A.; LeCraw, R. C. *J. Appl. Phys.* **1970**, *41*, 1218. (b) Day, P. *Acc. Chem. Res.* **1979**, *12*, 236.
(4) (a) Ohkoshi, S.; Mizuno, M.; Hung, G. J.; Hashimoto, K. *J. Phys. Chem. B*, **2000**, *104*, 9365. (b) Tozawa, M.; Ohkoshi, S.; Kojima, N.; Hashimoto, K. *Chem. Commun.* **2003**, 1204.
(5) (a) Kirk, M. L.; Rubie, N. D.; Hybl, L. *Polyhedron*, **2001**, *20*, 1741. (b) Garde, R.; Villain, F.; Verdaguer, M. *J. Am. Chem. Soc.* **2002**, *124*, 10538. (c) Ohba, M.; Iwamoto, T.; Okawa, H. *Chem. Lett.* **2002**, 1046. (d) Sato, Y.; Ohkoshi, S.; Hashimoto, K. *J. Appl. Phys.* **2002**, *92*, 4834.
(6) Fujita, W.; Awaga, K. *J. Am. Chem. Soc.* **1997**, *119*, 4563.
(7) (a) Burgess, J. *Metal Ions in Solution*; Ellis Horwood: New York, 1978. (b) Wilkins, R. G. *Kinetics and Mechanism of Reactions of Transition Metal Complexes*; VCH: Weinheim, Germany 1991. (c) Hathaway, B. J.; Lewis, C. E. *J. Chem. Soc. A* **1969**, 1183. (d) Inada, Y.; Sugimoto, K.; Ozutsumi, K.; Funahashi, S. *Inorg. Chem.* **1994**, *33*, 1875.
(8) (a) Shriver, D. F.; Brown, D. B. *Inorg. Chem.* **1969**, *8*, 42. (b) Beauvais, L. G.; Shores, M. P.; Long, J. R. *J. Am. Chem. Soc.* **2000**, *122*, 2763.

25 K.[9] In the present work, solvatochromic and solvato-magnetic effects in a cobalt hexacyanochromate were studied and drastic changes in color and magnetic properties were observed. Here, we report on a new magneto-optical functionality, *the solvatomagnetism-induced Faraday effect,* with a cobalt hexacyanochromate-based magnet.

2. Experimental Section

2.1. Materials. $Co^{II}_{1.5}[Cr^{III}(CN)_6]\cdot7.5H_2O$ (**1**) was prepared by adding 50 mL of an aqueous solution of $K_3[Cr(CN)_6]$ (10 mmol dm^{-3}) to 50 mL of $CoCl_2\cdot6H_2O$ aqueous solution (15 mmol dm^{-3}). The precipitated powder was washed with distilled water and air-dried. When the powder **1** was immersed in EtOH, the color drastically changed, which will be referred to as compound **2**.

2.2. Measurements. Elemental analyses of Co and Cr for compounds **1** and **2** were obtained by an HP4500 inductively coupled plasma mass spectroscopy (ICP-MS), and those of C, H, and N were determined using a standard microanalytical method. The visible reflectance spectra were measured using a Shimadzu UV-3100PC UV−vis spectrophotometer. The crystal structures of the samples were determined by a Rigaku RINT2100 X-ray powder diffraction (XRD) spectrometer. The infrared (IR) spectra were measured using a Shimadzu FTIR-8200PC. The magnetic properties were measured using a Quantum Design MPMS 7 superconducting quantum interference device (SQUID) magnetometer. Electron spin resonance (ESR) spectra were recorded with a JEOL RE1X X-band ESR spectrometer. The Faraday spectra were recorded on a JASCO E-250 magneto-optical meter. For the measurement of Faraday spectra, the fine powder type of sample spread on the CaF_2 substrate was used.

3. Results

3.1. Structure. Compound **1** was a peach powder. Elemental analyses by an ICP-MS and standard microanalytical methods confirmed that the formula of **1** was $Co^{II}_{1.5}[Cr^{III}(CN)_6]\cdot7.5H_2O$. Calculated: Co, 20.5; Cr, 12.1; C, 16.7; H, 3.5; N, 19.5%. Found: Co, 20.7; Cr, 12.3; C, 16.4; H, 3.5; N, 19.0%. When **1** was immersed in EtOH, its color changed to deep blue, as shown in Figure 1a. Successively, when this deep blue compound was immersed in H_2O, the color reverted to peach and this solvatochromic behavior was repeatedly observed several times. Elemental analyses showed that the formula of **2** was $Co^{II}_{1.5}[Cr^{III}(CN)_6]\cdot2.5H_2O\cdot2.0EtOH$. Calculated: Co, 20.4; Cr, 12.0; C, 27.7; H, 3.9; N, 19.4%. Found: Co. 20.5; Cr, 12.1; C, 27.4; H, 3.9; N, 19.5%. Figure 1b shows the visible reflectance spectra for **1** and **2**. Compound **1** possessed an absorption band around 490 nm (**A** band). In contrast, **2** possessed a different absorption band around 580 nm (**B** band) in addition to the **A** band. The IR spectra for **1** had a CN stretching peak at 2168 cm^{-1}, while **2** displayed a shoulder CN peak at 2166 cm^{-1}. In addition, **2** had CO stretching peaks due to the coordinating EtOH molecules at 1035 and 1085 cm^{-1}. The XRD patterns showed that both **1** and **2** were face-centered cubic (fcc) structures (Figure 2). The lattice constant, however, expanded from 10.583 (**1**) to 10.634 Å (**2**).

3.2. Magnetic Properties. The field-cooled magnetization plots of **1** in a magnetic field of 10 G showed a spontaneous
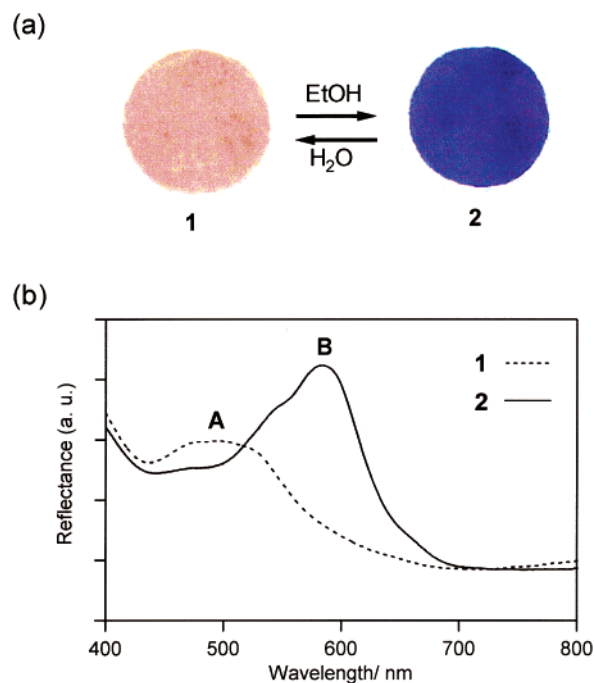

Figure 1. Photographs (a) and reflectance spectra (b) of **1** (dotted line) and **2** (solid line).
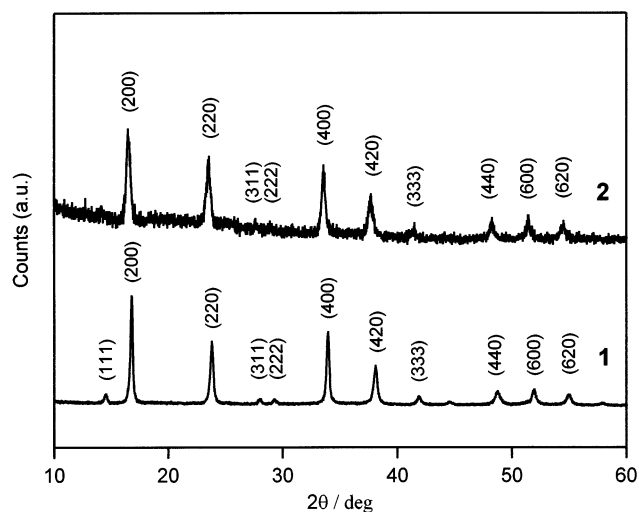
Figure 2. X-ray diffraction pattern spectra of **1** and **2** with Miller indices of face-centered cubic structure.

magnetization with a T_C of 25 K (Figure 3a). The magnetization versus external magnetic field at 5 K showed a saturation magnetization (M_s) value of 7.0 μ_B for a given formula of $Co^{II}_{1.5}[Cr^{III}(CN)_6]\cdot7.5H_2O$ (Figure 3b) and a coercive field (H_c) of 240 G (Figure 3c). The temperature dependence of magnetic susceptibility (χ) data showed that the Weiss constant (θ) of **1** was +32 K. Immersing in EtOH drastically altered the magnetic properties of the sample; that is, compound **2** had a T_C = 18 K, M_s = 5.5 μ_B, H_c = 120 G (Figure 3a−c), and θ = +21 K. Immersing **2** in water caused the magnetic properties to revert to **1**, which indicates that the observed solvatomagnetism between **1** and **2** is reversible. This switching behavior was repeatedly observed. ESR spectra showed that g-factors of **1** and **2** were 2.12 and 2.20, respectively.

(9) (a) Ohkoshi, S.; Hashimoto, K. *Chem. Phys. Lett.* **1999**, *314*, 210. (b) Verdaguer, M.; Bleuzen, A.; Marvaud, V.; Vaissermann, J.; Seuleiman, M.; Desplanches, C.; Scuiller, A.; Train, C.; Grade, R.; Gelly, G.; Lomenech, C.; Rosenman, I.; Veillet, P.; Cartier, C.; Villain, F. *Coord. Chem. Rev.* **1999**, *190*, 1023.
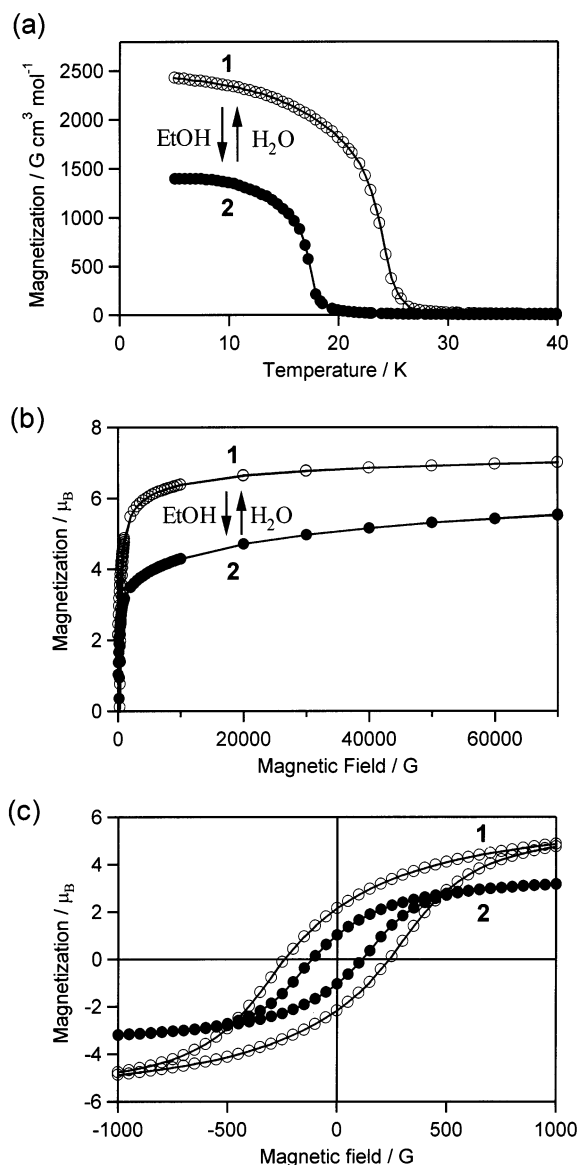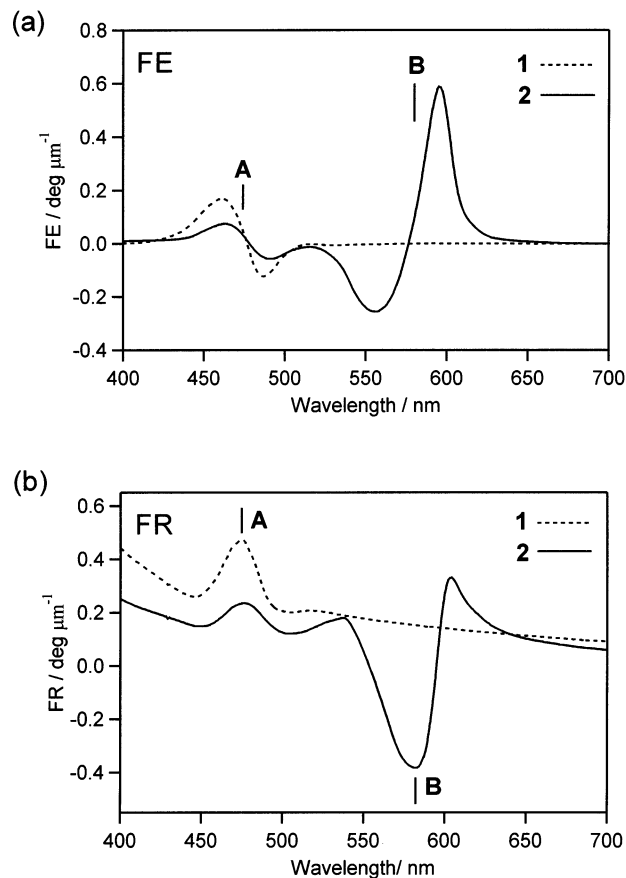
Figure 3. Magnetic properties of **1** (○) and **2** (●). (a) Field-cooled magnetization curves in an external magnetic field of 10 G. (b) Magnetization as a function of external magnetic field at 5 K. (c) Magnetic hysteresis loops at 5 K.

Figure 4. Faraday ellipticity (FE) (a) and Faraday rotation (FR) spectra (b) of **1** (dotted line) and **2** (solid line) collected at 7 K in an external magnetic field of 1 T.

3.3. Faraday Spectra. Figure 4 shows the Faraday spectra of **1** and **2** at 7 K in an external magnetic field of 1 T. The Faraday ellipticity (FE) spectrum of **1** had a distorted dispersive peak (**A**) around 480 nm with intensities of +0.17 deg μm^{-1} (460 nm) and −0.12 deg μm^{-1} (485 nm). Simultaneously, in the Faraday rotation (FR) spectrum, a positive bell-shaped peak was observed at the same position. In addition to the **A** band, the FE spectra of **2** displayed an intense dispersive-shaped band (**B**) with a center at 580 nm and had intensities of −0.26 deg μm^{-1} (555 nm) and +0.59 deg μm^{-1} (595 nm). The **B** band in the FR spectra showed a negative distorted wing-type peak with an intensity of −0.38 deg μm^{-1}(580 nm).

## 4. Discussion

4.1. Solvatochromic Property. In the $A^{II}_{1.5}[B^{III}(CN)_6]\cdot zH_2O$ type of Prussian blue analogues (A and B are transition metal

ions), vacancies randomly exist in the lattice as shown in Figure 5a. In these vacancies, an H_2O molecule coordinates to A^{II} ion as a *ligand water* instead of a nitrogen atom of a cyano group and the interior of vacancy is occupied by *zeolitic waters*. Since one-third of the $[Cr^{III}(CN)_6]$ sites are vacant in copound **1**, the Co^{II} ions are expected to coordinate to four N atoms of cyano groups and two O atoms of ligand waters on the average. The statistical probabilities of $Co^{II}N_6$ (geometry **I**), $Co^{II}N_5O$ (geometry **II**), $Co^{II}N_4O_2$ (geometry **III**), $Co^{II}N_3O_3$ (geometry **IV**), $Co^{II}N_2O_4$ (geometry **V**), and $Co^{II}NO_5$ (geometry **VI**) are expressed by the product of the combination ($_6C_n$; $n = 0-5$) and existing probabilities of $^1/_3$ and $^2/_3$ for O and N atoms, that is, $_6C_n\ (^1/_3)^n(^2/_3)^{6-n}$, where n is the number of O atoms. Moreover, the geometries of **III**, **IV**, and **V** are divided into two types (**a** and **b**) depending on coordinating positions of O atoms. As shown in Figure 5b, the statistical probabilities are estimated to be 8.8% (**I**), 26.4% (**II**), 26.4% (**III-a**), 6.6% (**III-b**), 13.2% (**IV-a**), 8.8% (**IV-b**), 6.6% (**V-a**), 1.6% (**V-b**), and 1.6% (**VI**). Here, the contribution of the surface for the existing probability can be neglected, since the particle size of microcrystal is large (ca. 500 nm). We also carried out the numerical calculation of probabilities on the computer, using $100 \times 100 \times 100$ atoms (1 million atoms) corresponding the cubic crystal with the size of 50 nm. As a result, the numerically calculated probabilities almost correspond to the statistical probability mentioned above. Figure 5c shows a schematic illustration of the solvent exchange between H_2O and EtOH on Co^{II} ion for
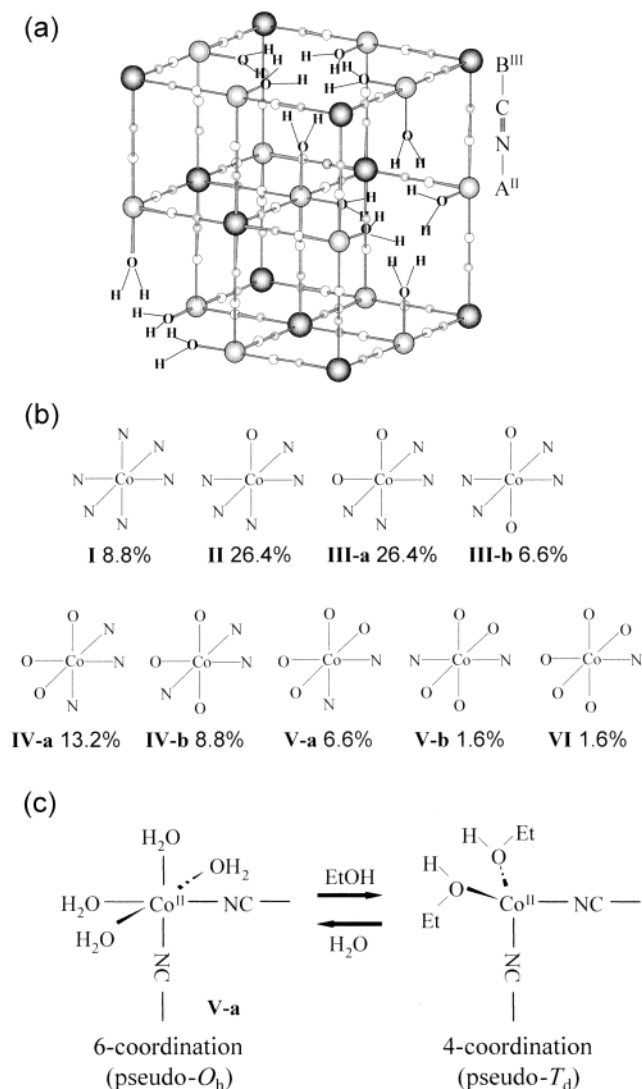
Figure 5. (a) Schematic illustration of the crystal structure of $A^{II}_{1.5}[B^{III}$-$(CN)_6]·zH_2O$. Ligand water molecules coordinate to A^{II} ions around the vacancies of $[B^{III}(CN)_6]$, and zeolitic water molecules (omitted in this figure) occupy the interior of the vacancies. (b) The statistical probabilities of possible coordinating geometries around Co^{II} ions. (c) Variation in the coordination geometry around Co^{II} by the solvent exchange for the coordination geometry of **V-a**. EtOH molecules substitute water molecules, changing the coordination geometry from six-coordination (pseudo-O_h) to four-coordination (pseudo-T_d).

geometry **V-a**. Co^{II} ions in steric bulky solvents prefer a tetrahedral geometry (T_d) over an octahedral geometry (O_h).[7,8] Moreover, it is reported that the optical transition of an octahedral coordinated Co^{II} (O_hCo^{II}) is around 490 nm with a small absorption coefficient and the optical transition of a tetrahedral coordinated Co^{II} (T_dCo^{II}) appears in the vicinity of 560 nm with a large absorption coefficient,[10] which are consistent with the observed reflectance spectra for **1** and **2**. Therefore, ligand substitution from H_2O to EtOH in **1** changed the coordination geometry of some of the Co^{II} ions from six-coordinate (pseudo-O_h) to four-coordinate (pseudo-T_d) geometries. Such a change is also expected at the sites of **IV-a** and **VI**. In other coordinate geometries such as **IV-b** and **V-b**,

(10) (a) Larrabee, J. A.; Alessi, C. M.; Asiedu, E. T.; Cook, J. O.; Hoerning, K. R.; Klingler, L. J.; Okin, G. S.; Santee, S. G.; Volkert, T. L. *J. Am. Chem. Soc.* **1997**, *119*, 4182. (b) Vallee, B. L.; Holmquist, B. *Methods for Determining Metal Ion Environments in Proteins: Structure and Function of Metalloproteins*; Elsevier/North-Holland: New York, 1980.
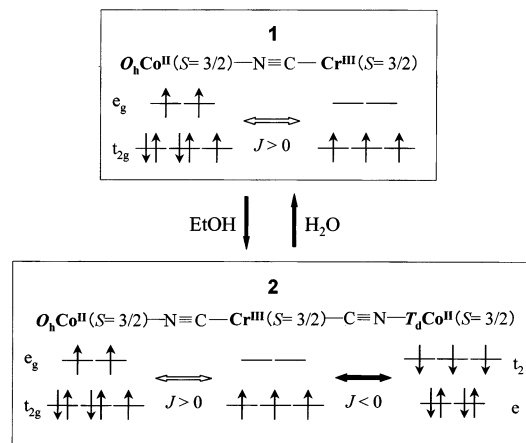

Figure 6. Explanation of solvatomagnetism in cobalt hexacyanochromate. Superexchange interactions of $O_hCo^{II}-NC-Cr^{III}$ and $T_dCo^{II}-NC-Cr^{III}$ are ferromagnetic ($J > 0$) and antiferromagnetic ($J < 0$), respectively.
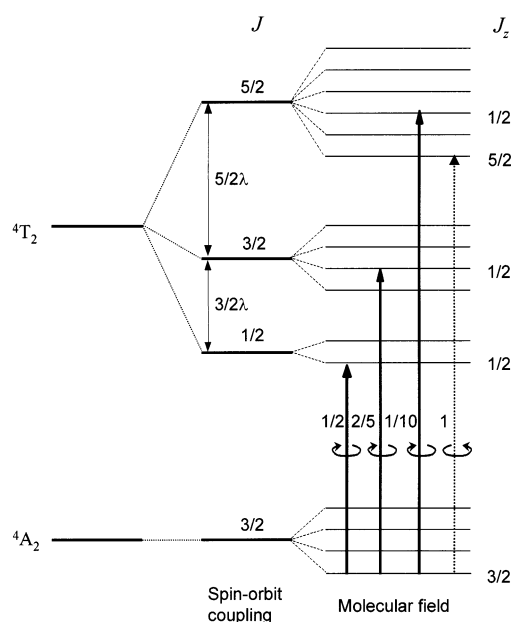
Figure 7. Multielectron energy diagram of $^4A_2 \rightarrow {}^4T_2$ transition on the T_dCo^{II} ion, with three allowed left circularly polarized light (solid vertical lines) and one allowed right polarized light (dashed vertical line). The numbers attached to each vertical line are the relative transition strengths calculated by the Wigner−Eckart theory.

obtaining the tetragonal coordinate is difficult because the ∠N−Co−N = 180° is contained in their geometries. When the ligand waters on sites of **IV-a**, **V-a**, and **VI** are substituted by EtOH molecules, the 21.4% portion of the Co^{II} ions in this compound is expected to be converted from six-coordinate to four-coordinate geometries.

4.2. Solvatomagnetic Property. The observed M_s value of 7.0 μ_B for **1** is close to the calculated value of 7.95 μ_B for the ferromagnetic coupling between the Co^{II} ($t_{2g}^5 e_g^2$, $S = {}^3/_2$) and Cr^{III} (t_{2g}^3, $S = {}^3/_2$) ions in a given formula and g-factor. In contrast, the M_s value of **2** (= 5.5 μ_B) is smaller than that of **1**, which indicates that the magnetic coupling between T_dCo^{II} and Cr^{III} is antiferromagnetic. Hence, compound **2** contains two superexchange interactions of ferromagnetic ($O_hCo^{II}-NC-Cr^{III}$) and antiferromagnetic ($T_dCo^{II}-NC-Cr^{III}$) (Figure 6). Thus, the magnetic properties of the present system obey a *mixed ferro−ferrimagnetism* as described in our previous papers.[11] The M_s
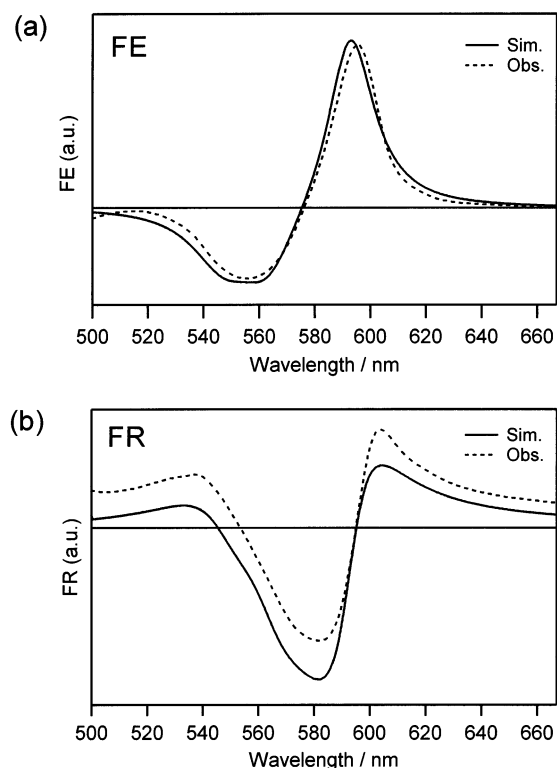
Figure 8. Simulation of Faraday spectra of **2** considering the ligand field splitting, spin—orbit coupling, and ferromagnetic ordering: (a) observed (dotted line) and simulated FE spectra (solid line) and (b) observed (dotted line) and simulated FR spectra (solid line).

value of $(T_dCo^{II}_x O_hCo^{II}_{1-x})_{1.5}[Cr^{III}(CN)_6]$ is expressed by eq 1,

$$M_S = |g_{Cr}S_{Cr} + 1.5[- g_{T_dCo}S_{T_dCo}x + g_{O_hCo}S_{O_hCo}(1 - x)]| \quad (1)$$

where spin quantum numbers of S_{Cr}, S_{T_dCo}, and S_{O_hCo} are $3/2$ and g-factors of g_{Cr}, g_{T_dCo}, and g_{O_hCo} are 2.00, 2.33, and 2.20, respectively. Based on this equation, the M_s value depends on x; for example, the M_s value for $x = 0.78$ is zero. The M_s value of 5.5 μ_B for **2** suggests that the estimated x value is 0.24. This x value is close to the sum value ($= 21.4\%$) of the theoretical probabilities of **IV-a**, **V-a**, and **VI** in T_dCo^{II} in section 4.1. The decrease of θ value from +32 K (**1**) to +21 K (**2**) also obeys the theory of the mixed ferro—ferrimagnetism.[11c] Therefore, it is concluded that the appearance of the antiferromagnetic contribution between T_dCo^{II} and Cr^{III} ions caused the solvatomagnetism.

4.3. Solvatomagnetism-Induced Faraday Effect. In both FE spectra of **1** and **2**, a dispersive **A** band centered at 470 nm was observed as shown in Figure 4. Judging from its position, we assigned the **A** band to $^4T_{1g} \rightarrow {}^4T_{1g}$, $^2T_{1g}$ transitions on the O_hCo^{II} ion.[10] In contrast, the **B** band of **2** is assigned to the $^4A_2 \rightarrow {}^4T_2$ transition of the T_dCo^{II} ion. The absorption coefficient of the T_dCo^{II} ion is known to be 10—50 times as much as the value of the O_hCo^{II} ion.[10] Along with these assignments, a spectral simulation, which considered the ligand field splitting, spin—orbit coupling, and the ferromagnetic ordering, was conducted. Figure 7 shows the multielectron energy diagram of the $^4A_2 \rightarrow {}^4T_2$ transition in an ideal T_dCo^{II} ion. The excited

(11) (a) Ohkoshi, S.; Iyoda, T.; Fujishima, A.; Hashimoto, K. *Phys. Rev. B* **1997**, *56*, 11642. (b) Ohkoshi, S.; Abe, Y.; Fujishima, A.; Hashimoto, K. *Phys. Rev. Lett.* **1999**, *82*, 1285. (c) Ohkoshi, S.; Hashimoto, K. *Phys. Rev. B* **1999**, *60*, 12820.

state is equivalent to the $^4P(L = 1)$ state, and then the spin—orbit coupling splits it into three levels, which are determined by the total angular momenta $J = 5/2$, $3/2$, and $1/2$. In a ferromagnetic state, the molecular field further splits each J level into $2J + 1$ levels specified by J_z and the optical transitions are only from the lowest $J_z = 3/2$ state in the ground state. The transition strengths for left or right circularly polarized light can be evaluated by the Wigner—Eckart theory. The vertical lines in Figure 7 show the allowed transitions and the relative transition strengths. The frequency (ω) dependencies of the FE and FR angles for each transition are calculated by eqs 2 and 3.

$$FE \cong \frac{Ne^2\gamma\Delta f\omega_0}{m\epsilon_0\{(\omega_0^2 - \omega^2 + \gamma^2)^2 + 4\omega^2\gamma^2\}} \quad (2)$$

$$FR \cong -\frac{Ne^2\Delta f(\omega_0^2 - \omega^2 + \gamma^2)\omega_0}{2m\epsilon_0\omega\{(\omega_0^2 - \omega^2 + \gamma^2)^2 + 4\omega^2\gamma^2\}} \quad (3)$$

where N is the number of ions per unit volume, e is the charge of an electron, Δf is the relative transition strengths, ω_0 and γ are the absorption center and half width of each transition, respectively, m is the weight of electron, and ϵ_0 is the dielectric permeability in a vacuum. To simulate the Faraday spectra of **2**, the following values were used: $\omega_0 = 17\,400$ cm^{-1}, $\lambda = 350$ cm^{-1}, and $\gamma = 300$ cm^{-1} ($J = 5/2$), 400 cm^{-1} ($J = 3/2$), and 500 cm^{-1} ($J = 1/2$). The shape of the calculated FE and FR spectra well reproduced the observed spectra as shown in Figure 8a and b, respectively.

5. Conclusion

In this paper, a solvatomagnetism-induced Faraday effect in cobalt hexacyanochromate is proposed. This effect is due to ligand substitution, which causes a change in the coordination geometry around Co^{II} ions ($O_hCo^{II} \leftrightarrow T_dCo^{II}$) and switches of the magnetic interaction from ferromagnetic coupling ($O_hCo^{II}-Cr^{III}$) to antiferromagnetic coupling ($T_dCo^{II}-Cr^{III}$). One target in the field of molecule-based magnets is to achieve new magnetic optical functionalities such as magneto-optics[4,5] and photomagnetism.[12] Among molecule-based magnets, cyanide-bridged metal complexes[9b,13–15] are useful systems in designing new magneto-optical functionalities. Recently, we have observed the photoinduced Faraday effect as one of new magneto-optical functionalities.[5d] Moreover, we are now

(12) (a) Sato, O.; Iyoda, T.; Fujishima, A.; Hashimoto, K. *Science* **1996**, *272*, 704. (b) Ohkoshi, S.; Yorozu, S.; Sato, O.; Iyoda, T.; Fujishima, A.; Hashimoto, K. *Appl. Phys. Lett.* **1997**, *70*, 1040. (c) Bleuzen, A.; Lomenech, C.; Escax, V.; Villain, F.; Varret, F.; Moulin, C. C. D.; Verdaguer, M. *J. Am. Chem. Soc.* **2000**, *122*, 6648. (d) Ohkoshi, S.; Machida, N.; Zhong, Z. J.; Hashimoto, K. *Synth. Met.* **2001**, *122*, 523. (e) Rombaut, G.; Verelst, M.; Golhen, S.; Ouahab, L.; Mathoniere, C.; Kahn, O. *Inorg. Chem.* **2001**, *40*, 1151. (f) Pejaković, D. A.; Kitamura, C.; Miller, J. S.; Epstein, A. J. *Phys. Rev. Lett.* **2002**, *88*, 057202−1. (g) Tokoro, H.; Ohkoshi, S.; Hashimoto, K. *Appl. Phys. Lett.* **2003**, *82*, 1245. (h) Arimoto, Y.; Ohkoshi, S.; Zhong, Z. J.; Seino, H.; Mizobe, Y.; Hashimoto, K. *J. Am. Chem. Soc,* **2003**, *125*, 9240.
(13) (a) Miller, J. S. *MRS Bull.* **2000**, *25*, 60. (b) Hashimoto, K.; Ohkoshi, S. *Philos. Trans. R. Soc. London, Ser. A* **1999**, *357*, 2977. (c) Ohba, M.; Okawa, H. *Coord. Chem. Rev.* **2000**, *198*, 313.
(14) (a) Griebler, W. D.; Babel, D. Z. *Naturforsch., B* **1982**, *87*, 832. (b) Mallah, T.; Thiebaut, S.; Verdaguer, M.; Veillet, P. *Science* **1993**, *262*, 1554. (c) William, R. E.; Girolami, G. S. *Science* **1995**, *268*, 397. (d) Ferlay, S.; Mallah, T.; Ouahs, R.; Veillet, P.; Verdaguer, M. *Nature* **1995**, *378*, 701. (e) Holmes, S. M.; Girolami, G. S. *J. Am. Chem. Soc.* **1999**, *121*, 5593. (f) Hatlevik, Ø.; Bushmann, W. E.; Zhang, J.; Manson, J. L.; Miller, J. S. *Adv. Mater.* **1999**, *11*, 914.

studying the humidity control of the magneto-optical effect with the present system. Since new building blocks for cyanide-bridged metal complexes are currently being prepared,[16] various additional magneto- optical functionalities will be observed with molecule-based magnets soon.

(15) (a) Garde, R.; Desplanches, C.; Bleuzen, A.; Veillet, P.; Verdaguer, M. *Mol. Cryst. Liq. Cryst*. **1999**, *334*, 587. (b) Zhong, Z. J.; Seino, H.; Mizobe, Y.; Hidai, M.; Fujishima, A.; Ohkoshi, S.; Hashimoto, K. *J. Am. Chem. Soc.* **2000**, *122*, 2952. (c) Larionova, J.; Gross, M.; Pilkington, M.; Andres, H.; Stoeckli-Evans, H.; Güdel, H. U.; Decurtins, S. *Angew. Chem., Int. Ed.* **2000**, *39*, 1605. (d) Zhong, Z. J.; Seino, H.; Verdaguer, M.; Ohkoshi, S.; Hashimoto, K. *Inorg. Chem.* **2000**, *39*, 5095. (e) Podgajny, R.; Korzeniak, T.; Balanda, M.; Wasiutynski, T.; Errington, W.; Kemp, T. J.; Alcock, N. W.; Sieklucka, B. *Chem. Commun.* **2002**, 1138.

(16) (a) Beauvais, L. G.; Long, J. R. *J. Am. Chem. Soc*. **2002**, *124*, 2110. (b) Lescouëzec, R.; Vaissermann, J.; Lloret, F.; Julve, M.; Verdaguer, M. *Inorg. Chem.* **2002**, *41*, 5943. (c) Bennett, M. V.; Long, J. R. *J. Am. Chem. Soc.* **2003**, *125*, 2394. (d) Smith, J. A.; Galán-Mascarós, J. R.; Clérac, R.; Sun, J. S.; Ouyang, X.; Dunbar, K. R. *Polyhedron*, **2001**, *20*, 1727.